Confined Single Alkali Metal Ion Platform in Zeolite Pore for Concerted Benzene C–H Activation-to-Phenol Catalysis

Shilpi Ghosh[†], Shankha S. Acharyya[†], Takuma Kaneko[†], Kotaro Higashi[†], Yusuke Yoshida[†], Takehiko Sasaki[‡] and Yasuhiro Iwasawa[*,†,§]

[†] Innovation Research Center for Fuel Cells, The University of Electro-Communications, Chofu, Tokyo 182-8585, Japan
[‡] Graduate School of Frontier Science, The University of Tokyo, Kashiwa, Chiba 277-8561, Japan
[§] Graduate School of Informatics and Engineering, The University of Electro-Communications, Chofu, Tokyo 182-8585, Japan

Supporting Information Placeholder

ABSTRACT: The well-known cumene process via an explosive cumene hydroperoxide intermediate in liquid phase currently employed for phenol production is energy-intensive and not environmentally friendly. Therefore, there is a demand for an alternative single-step gas-phase catalysis process. According to the conventional catalysis concept, selective oxidation reactions are promoted by redox catalysts and not by acid–base catalysts. In general, alkali and alkaline-earth metal ions cannot activate each of benzene, O_2 and N_2O when they adsorb separately. However, we observed an unprecedented catalysis of single alkali and alkaline earth metal ion sites incorporated into zeolite pores for the selective oxidation of benzene to phenol with N_2O and O_2+NH_3, thereby providing a single-site catalytic platform with high selectivity. Among alkali and alkaline earth metal ions, single Cs^+ and Rb^+ sites with ion diameters of > 300 pm in the pores of β zeolites exhibited remarkable selectivity for benzene C–H activation-to-phenol catalysis in a concerted reaction pathway.

KEYWORDS: Concerted benzene C-H functionalization, Selective phenol synthesis, Confined single site catalysis, Alkali and alkaline-earth metal ions/zeolite.

1. INTRODUCTION

Phenol is an important industrial precursor (~10 megaton/year) for producing various polymers (nylon, phenolic resins, etc.), drugs, herbicides, and detergents. It is industrially produced via the energy-intensive and environmentally harmful cumene process.[1] This process is implemented in three steps, and it involves an explosive cumene hydroperoxide intermediate, requires sulfuric acid to decompose into equimolar amounts of phenol and acetone in liquid phase, and suffers from the disadvantage of low yield. Although the cumene process has been widely employed for phenol production for a long time, an alternative method for the direct synthesis of phenol from benzene with O_2 and N_2O in a single-step gas-phase flow reaction on a solid catalyst is desirable from the perspectives of achieving high atomic efficiency, reduction of energy and resource consumption, and the ease of product separation.[2]

According to the conventional concept of catalysis, selective oxidation reactions do not proceed significantly on acid–base catalysts, such as zeolites, ion-exchanged resins, Brønsted and Lewis acidic/basic metal oxides, and heteropoly acids,[3-13] but they proceed on redox catalysts, such as precious and transition metals, reducible metal oxides, metal sulfides, and supported metal complexes.[3-13]. Typically, the gas-phase selective oxidation of benzene to phenol with O_2, N_2O and H_2/O_2 has been observed with metal and metal oxide catalysts of V, Fe, Ni, Cu, Mo, Pd, W, Re, Ir, Pt, etc.[14-37] These catalysts possess moderate redox potentials and sufficient M–O bond strengths to provide active lattice oxygen and reactive oxygen intermediates.[14-37] Except these classifications, there are rare reports on photo-oxidation of hydrocarbons and N_2O_4 decomposition using alkali and alkaline-earth metal/zeolite catalysts.[38-41]

Meanwhile, in contrast to the traditional catalysis concept, we discovered the unprecedented catalysis of the large alkali metal (Cs and Rb) ions incorporated in β zeolite pores with weak acid–base properties for the selective oxidation of benzene to phenol with N_2O (99.9% selectivity at 25.5% one-path conversion on 0.4 g_{cat}) and O_2 (+NH_3) (85.1% selectivity at 6.3% one-path conversion on 0.6 g_{cat}); in this process, large Cs^+ and Rb^+ single sites provide a catalysis platform for the benzene C–H activation toward phenol synthesis from benzene and N_2O or from benzene and O_2 in the presence of NH_3.

Alkali and alkaline-earth metal ions cannot activate each of benzene, O_2 and N_2O when they adsorb separately. However, alkali and alkaline earth metal cations/β zeolite catalysts, examined via XPS, STEM-EDS and *in situ* XAFS and through DFT calculations, selectively promoted benzene C–H activation toward direct phenol synthesis, providing the pivotal single metal ion site platform confined in β zeolite pore for a selective inter-ligand concerted reaction pathway that differs from traditional redox catalysis. The present findings present a new ap-

proach for designing efficient selective C–H activation catalysis under mild conditions.

2. EXPERIMENTAL SECTION

Chemicals. High Purity helium (>99.999 vol %, Taiyo Nippon Sanso), oxygen (>99.999 vol %, Taiyo Nippon Sanso), ammonia (>99.999 vol %, Showa Denko), N2O (>99.999 vol%, ShowaDenko) and methane (>99.999 vol %, Taiyo Nippon Sanso) in high pressure cylinders were purchased from the manufacturers and used without further purification. Benzene, metal salts and β zeolite were purchased from Wako chemicals, Kanto Chemical Co., and JGCC &C, respectively.

Catalyst preparation. Zeolite β-supported metal ion catalysts (M/β: M=Na, Mg, K, Ca, Rb, Sr, Cs, Ba, V, Cr, Mn, Fe, Co, Ni, Cu, Ag and Ir) were prepared by ion-exchange method using corresponding metal nitrates salts as precursors. Typically, Rb(1 wt %)/β was synthesized as follows: 0.172 g of RbNO3 (Wako chemicals) was dissolved in 25 Ml Milli-Q water, to which solution 9.9 g of β zeolite withSiO_2/Al_2O_3 = 25 was added under stirring. Thereafter, the solution was suspended for 12h at 353 K for ion-exchange. Next, the suspension was filtered under a reduced pressure and with deionized water (500 mL) three times, followed by the treatment at 353 K for 6h. As another typical example, Cs (2.1 wt %) /β was synthesized as follows. 0.062 g of $CsNO_3$ (Kanto Chemical Co.) was dissolved in 10 mL deionized water in a 50 mL Erlenmeyer flask, to which solution 1.96g NH_4-β with SiO_2/Al_2O_3 = 25 was added under stirring. For ion-exchange of NH_4 ions with Cs ions, the solution was heated from room temperature to 353 K, and was maintained at 353 K for 12 h under stirring, followed by filtration under a reduced pressure and washing with deionized water (500 mL) three times, and finally drying at 353 K for 6h.

Catalytic reaction set-up and product analysis. Catalytic reactions were carried out in a tubular fixed-bed down-flow reactor (quartz tube O.D. 6 mm) at atmospheric pressure. The reactor tube was mounted inside a furnace and the thermocouple (K type) was aligned along the tube center in such a way that its tip reached the center of the catalyst bed. Zeolite particles (typically, 0.4 g, sieved into 500-850 μm particles) were packed between quartz wools. All gas lines were heated at 423 K to avoid condensation of the products. In the case of benzene/N_2O reaction systems, prior to the reaction, the temperature was raised to the reaction temperature (typically, 573 K) at a He flow rate of 20 mL min^{-1} in 30 min, then at 573 K the catalytic reaction was started under flows of benzene (0.5 mL min^{-1}), N_2O (3.0 mL min^{-1}), and methane (5.0 mL min^{-1}). Methane was used as an internal standard because methane never reacts on the examined catalysts in the present system. In the case of benzene/O_2/NH_3 reactions, the catalyst charged in a continuous down-flow fixed-bed flow glass reactor was also pretreated at 673 K for 0.5 h in a flow of Bz/O_2/NH_3/He = 0.5/0.5/1.8/4.0 mL min^{-1} and cooled rapidly to a reaction temperature (e.g. 593 K). The conversion and selectivity in the Bz+O_2+NH_3 system were calculated by using NH_3 as an internal standard taking into account the calibration factors for NH_3 in the FID and TCD GCs in a similar way to that in our previous reports (Refs. 15 & 16). The outlet stream was sampled with six-way sampling valves heated at 423 K every 30 min using on-line Shimadzu GC-2014 with a FID using a ZB-WAX plus capillary column (30 m, Phenomenex CA USA) for CH_4, NH_3, benzene and phenol, and Shimadzu GC-2014 with a TCD using a WG-100 column (GL Science Japan) for O_2, N_2, CO, CO_2, CH_4, N_2O, NH_3 and H_2O. Helium was used as carrier gas. The column temperature for TCD was 313K. The column temperature for FID was held at 351 K for 5 min, and then increased to 453 K at a heating rate of 288 K min^{-1}. The quantitation of ammonia decomposition products (only N_2 was always detected by GC) was calculated by the equation, NH_3 decomposition (%) = $(CF_{N2} \times [N_2]_{TCD\text{-}GC} \times 2) \times 100/[(CF_{N2} \times [N_2]_{TCD\text{-}GC} \times 2) + (CF_{NH3} \times [NH_3]_{TCD\text{-}GC})]$, where CF_{N2} (calibration factor for N_2) and CF_{NH3} (CF for NH_3) were 2.00×10^{-11} and 3.00×10^{-11}, respectively. The elemental carbon and nitrogen mass balances in the Bz+N_2O and Bz+O_2+NH_3 systems based on the inlet flows of benzene and N_2O or NH_3 were examined to be the values between 97% and 100% in most of the experimental runs.

***In situ* XAFS measurements and XAFS data analysis.** *In situ* XAFS spectra at Cs L3-edge and Rb K-edge for Cs/β and Rb/β, respectively were measured at 15 K in a fluorescence mode at BL36XU station in SPring-8. XANES and EXAFS spectra were analyzed in the similar way to the previous reports,[42] using the Larch code containing the IFEFFIT Package ver.2 (Athena and Artemis).[43] Background subtraction in the EXAFS analysis was performed using Autobk.[44] The Victoreen function was employed for the background subtraction and the spline smoothing method with Cook and Sayers criteria was used as the μ_0 method. The extracted k^2-weighted EXAFS oscillations were Fourier-transformed to R-space over k = 25–80 nm^{-1}, and the curve fittings were performed in the R-space (0.18–0.32 nm). The fitting parameters for each shell were coordination number (CN), inter-atomic distance (R), Debye-Waller factor (σ^2), and correction-of-edge energy (ΔE_0). The phase shifts and amplitude functions for Cs–O and Rb–O were calculated from the FEFF 8.4 code.[45] Error ranges of the curve-fitting analysis of EXAFS Fourier transforms were based on the definition of the Larch code.[43]

DFT calculations. All calculations were conducted with Dmol3 ver 3.0 (Accelrys, USA).[46] Numerical basis set with polarization function (DNP), of which quality is comparable to 6-31G*, was adopted. All electrons were explicitly included. All possible multiplicities of electronic states were compared in the calculations and optimized multiplicity was determined in each system. Perdew-Wang 91 functional (PW91).[47] was used in all the calculations. Transition states were searched by Dmol3 with the complete QST/LST option, where the Linear Synchronous Transit (LST) maximization was performed for the coordinates interpolated between a reactant and a product, followed by repeated conjugated gradient minimizations and the Quadratic Synchronous Transit (QST) maximizations until a transition state has been located.[48] In order to include the effect of zeolite framework, a cluster containing 10 Si and O atoms with neighboring 5-membered ring-4-membered ring–5 membered ring structure was taken from the crystal structure of β-zeolite with hydrogen atom-termination. One Si atom was replaced by Al atom with adding H atom on the neighboring oxygen atom. Positions of Al atom, the added H atom and neighboring oxygen atoms were relaxed by the structural optimization. Then the H atom was replaced by Cs atom and the structure was relaxed. Adsorption of benzene, O_2 and NH_3 and adsorption of benzene and N_2O and subsequent intermediate states and transition states were calculated.

3. RESULTS AND DISCUSSION

3.1 Selective oxidation of benzene with N_2O on single alkali and alkaline-earth metal-ion sites.

We observed the unexpected catalytic property of alkali and alkaline earth metal/zeolite catalysts for the selective oxidation of benzene with N_2O to form phenol at atmospheric pressure. Alkali and alkaline earth metal ions such as Mg^{2+}, K^+, Ca^{2+}, Rb^+ and Cs^+ incorporated into β zeolite pores showed good catalytic activities (13.6-18.9 one-path conv.% on 0.4 g_{cat} (metal loading: 1.0 wt%) at 573 K) for the selective phenol production with a tremendous selectivity of 99.9% (Table 1). The most active catalyst was Rb/β, which showed high one-path conversions of 24.3% on 0.5 g_{cat} at 573 K and 25.5% on 0.4 g_{cat} at 613 K, thus maintaining the 99.9% selectivity. The consumption/decomposition rate of N_2O decreased in the follownig order of catalysts Ca/β >K/β >Mg/β >Rb/β >Cs/β. The N_2O consumption on Rb/β and Cs/β was nearly stoichiometric to the phe nol production (Table 1). In other words, the catalytic process proceeded stoichiometrically in the following manner: benzene + N_2O → phenol + N_2 without extra N_2O decomposition. The decomposition conversion of N_2O alone without benzene on Rb/β was only 0.3%; further excessive N_2O decomposition was restricted in the presence of the coexisting benzene in the phenol synthesis process (Table 1). These results indicate the remarkable property of the Rb/β and Cs/β catalysts in practical applications. The catalytic reactions on the Rb/β and Cs/β proceeded steadily during time-on-stream of 250 min without deactivation as shown in Figure 1 (a & b). The performance depends on the following types of zeolites; Cs/Mordenite and Cs/ZSM-5 afforded phenol at very low conversions of 0.5% and 0.9%, respectively and they led to high undesirable N_2O decomposition, which was as large as $[N_2O]_{reacted}/[phenol]_{produced}$=5.7 and 47.1, respectively. Cs/faujasite Y showed no activity for the benzene hydroxylation (Table 1). Note that no reaction occurred when amorphous SiO_2-Al_2O_3 was used as the support for Cs (Cs/SiO_2-Al_2O_3 in Table 1). The remarkable property of Rb/β and Cs/β to show the 99.9% selectivity for benzene C–H functionalization to phenol synthesis with N_2O can be attributed to the large ion diameters of 0.304 nm and 0.334 nm for Rb^+ and Cs^+, respectively, and the confinement and local coordination structures of single Rb and Cs ion sites regulated by the β pore structure. The previous literature data for the gas-phase catalytic phenol synthesis from benzene on transition metal catalysts are listed in Table S1 as reference.

Table 1. Performances (conversion and selectivity) of various alkali and alkaline-earth metal/β zeolite catalysts and reference samples for the selective oxidation of benzene to phenol with N_2O [†]

Catalyst	Benzene conv./%	Phenol selec./%	N_2O decomp. conv./%	$[N_2O]_{reacted}/[Phenol]_{produced}$
Mg(1 wt%)/β [a]	14.1	99.9	3.2	1.2
K(1 wt%)/β [a]	13.6	99.9	3.4	1.5
Ca(1 wt%)/β [a]	14.4	99.9	4.9	2.0
Rb(1 wt%)/β [a]	18.9	99.9	3.2	1.0
Rb(1 wt%)/β [b]	24.3	99.9	4.3	1.0
Rb(1 wt%)/β [c]	25.5	99.9	4.3	1.0
Rb(1 wt%)/Hβ [a,d]	19.6	94.5	3.3	1.1
Rb(1 wt%)/β [a,e]	16.7	97.3	3.2	1.2
Rb(1 wt%)/β[f]	-	-	0.3	-
Cs(1 wt%)/β [a]	17.0	99.9	2.9	1.0
Cs(1 wt%)/ Mordenite [a]	0.5	99.9	0.5	5.7
Cs(1 wt%)/Y [a]	0	0	0	-
Cs(1 wt%)/ZSM-5 [a]	0.9	52.5	3.6	47.1
Cs(1 wt%)/ SiO_2-Al_2O_3[a]	0	0	0	-

[†] conv.: conversion; selec.: selectivity; decomp.: decomposition of N_2O to N_2. [a] Cat= 0.4 g (Metal loading=1.0 wt%), Reac. temp= 573 K; Performance values: averaged during 30-150 min time-on-stream. Benzene/N_2O/CH_4/He=0.5/3.0/5.0/20 mL min^{-1}; CH_4 was used as internal standard because it was inert under the present conditions. . [b] identical condition to [a] except for catal. weight=0.5 g. [c] identical condition to [a] except for reac. temp. 613 K. [d] H type β zeolite. [e] Pretreated at 673 K for 30 min before use as catalyst. [f] N_2O/He=3.0/25.5 mL min^{-1}.

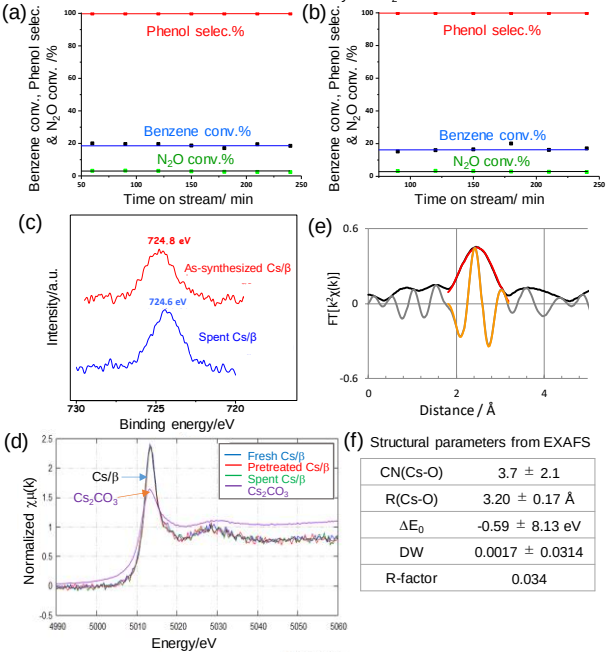

(f) Structural parameters from EXAFS

CN(Cs-O)	3.7 ± 2.1
R(Cs-O)	3.20 ± 0.17 Å
ΔE_0	-0.59 ± 8.13 eV
DW	0.0017 ± 0.0314
R-factor	0.034

Figure 1. Catalytic performances (benzene conversion, phenol selectivity and N_2O conversion) and XPS and XAFS characterizations of Cs/β and Rb/β catalysts. (a & b) Time-on-streams of the benzene+N_2O reactions on Rb/β catalyst (a) and of Cs/β catalyst (b). Catal. weight = 0.4 g; metal loading =1 wt%; react. Temp.= 573 K; Benzene/N_2O/CH_4/He = 0.5/3.0/5.0/20 mL min^{-1}. (c) *Ex situ* XPS spectra at Cs $3d_{5/2}$ for fresh (as-synthesized) and spent Cs (2 wt%)/β catalysts. (d) *In situ* Cs L_3-edge XANES spectra for fresh, pretreated and spent Cs/β catalysts and *ex situ* XANES spectrum for Cs_2CO_3. (e) *In situ* EXAFS Fourier transform (black: obs.; red: fitting; gray: imaginary part; orange: fitting). (f) structural parameters for the pretreated Cs/β determined by EXAFS curve-fitting analysis.

The *ex situ* XPS spectra at the $3d_{5/2}$ level for the as-synthesized (fresh) and spent (after the catalytic reaction) Cs/β catalysts in Figure 1 (c) revealed the binding energies of 724.8 and 724.6 eV, respectively, which resemble 724.8 eV for Cs_2CO_3 on Ag and 724.5 eV for CsOH. This suggests the presence of monovalent Cs^+ species in β pores.[49] The *in situ* Cs L_3-XANES spectrum for the as-synthesized Cs/β catalyst did not change with pretreatment before its application as a catalyst and also remained unchanged after the catalysis, as shown in Figure 1 (d). The edge energies for the as-synthesized, pretreated and spent Cs/β catalysts were all 5012.0 eV, which is the same as the energy for Cs_2CO_3 with Cs^+ valence. However, the white line peak intensity of the fresh and spent Cs/β catalysts greatly exceeded that of Cs_2CO_3. This result is inconsistent with the XPS results. We simulated the white line peak intensity for the Cs L_3-edge XANES by FEFF8.4[42–45] and found that the white line peak intensity at Cs L_3-edge strongly depends on the local coordination structure around the Cs ion. The FEFF simulation using the coordination structure around Cs ion was conducted based on DFT calculations with Dmol3 ver 3.0 (Accelrys).[46-48] The simula

tion results confirmed considerably larger peak intensity for the Cs/β than that for Cs_2CO_3. The EXAFS analysis at Cs L_3-edge for the pre-treated Cs/β sample before its use as a catalyst revealed only Cs–O bonds at 0.320 nm (±0.017 nm) with coordination number of 3.7 ±2.1, and no Cs–Cs bonds were detected as shown in Figure 1 (e & f). This observation suggests that a single Cs^+ site coordinated by three to four O atoms of the β pore wall acted as the active platform for the selective phenol synthesis from benzene and N_2O. Figure S2 shows bright and dark fields STEM images and elements (Si, O and Cs) mapping for Cs(2 wt%)/β. The STEM images reveal no feature except for the β zeolite lattice.

The XANES spectra for the as-synthesized and spent Rb/β catalysts were identical, and the edge energies were similar to that for Rb^+NO_3 aq., although determining the accurate value for the latter is difficult because of the overlapping of the pre-edge and white line peaks (Supporting information Figure S1). Again, the Rb K-edge EXAFS analysis for the Rb/β revealed no Rb–Rb bonds; only Rb–O bonds at 0.299–0.328 nm (±0.016nm) were observed. These results also charβ pores. The single Rb^+ and Cs^+ sites were not aggregated to Rb oxides

and Cs oxides under the catalysis conditions and upon increasing the Rb and Cs loadings as suggested from the XRD patterns shown in Figure S3; Rb(4 wt%)/β and Rb(8 wt%)/β with the higher Rb loadings showed no peaks other than β zeolite.

Figure 2 shows the plots of the benzene one-path conversion (%), phenol selectivity (%), and phenol yield (%) for benzene hydroxylation with N_2O at 573 K against the ionic radii of alkali (red mark) and alkaline earth (blue mark) metal ions. Inserted figure is a computanional coadsorption arrangement on a Cs^+ ion incorporated in β pore for benzene and N_2O by DFT calculations. The conversion and yield increased with larger alkali metal ion radii for radii larger than ~150 pm. Hence, for comparison, we also examined the performances of transition metal ions incorporated into β pores, but these ions did not show any significant activities for the selective benzene hydroxylation;

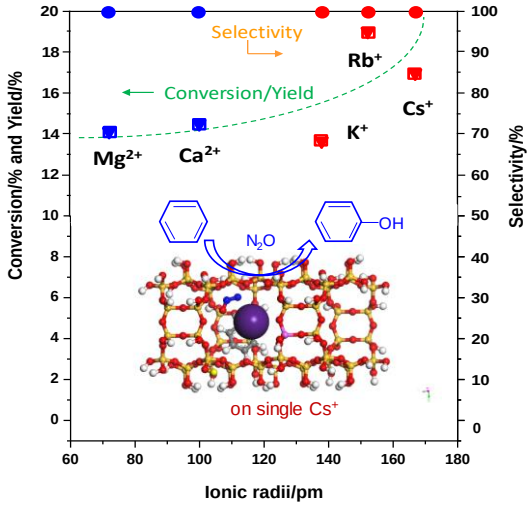

Figure 2. Plots of the benzene conversion(%), phenol selectivity(%), and phenol yield(%) for benzene hydroxylation with N_2O versus the ionic radii of alkali (red mark) and alkaline earth (blue mark) metal ions. Reac. temp.; 573 K. Benzene/N_2O/methane = 0.5/3.0/5.0 mL min^{-1}. Inseted figure is a computanional coadsorption arrangement on a Cs^+ ion incorporated in β pore for benzene and N_2O by DFT calculations.

Fe^{3+}/β showed typically low conversion (1.4%) and selectivity (17.9%), and there was considerable undesirable N_2O decomposition with $[N_2O]_{reacted}/[Phenol]_{produced} = 68.3$.

We conducted temperature programmed desorption (TPD) of CO_2 and acetonitrile (CH_3CN) on Cs/β and Rb/β at 300–923 K to estimate basic and acidic strengths, respectively (Figure S4). Most of the adsorbed CO_2 desorbed below 313 K, and the desorbed amount was negligible (< 1% of Cs and Rb), thus indicating very weak or negligible basicity of Cs/β and Rb/β. The TPD peaks for CH_3CN on Cs/β and Rb/β were observed around 365 K and 348 K, respectively, and the desorbed CH_3CN amounts per Cs and Rb (after subtracting the desorbed amount from β) were 57%–75% of the alkali metal quantity (Figure S4). These results indicate the weak acidity of single Cs and Rb ions in β pores. Therefore, the single Cs^+ and Rb^+ sites possess the characteristic of a weak Lewis acid.

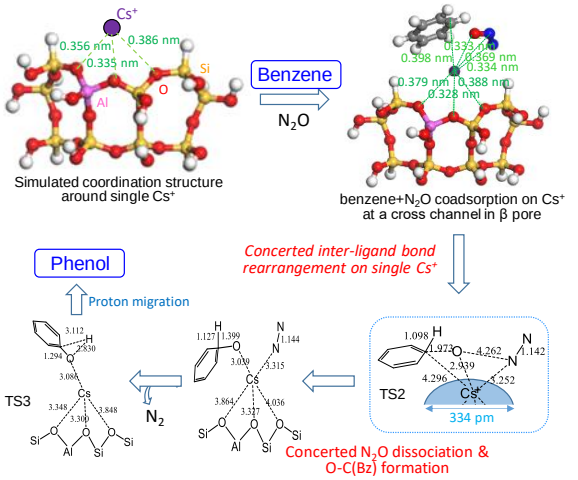

Figure 3. Associative Bz+N_2O coadsorption, concerted O–C(benzene) bond formation and transition states (TS1 and TS2) in a computational reaction pathway on single Cs^+ site at a cross channel arrangement in β zeolite pore.

To understand the key factor and mechanism for benzene C-H activation to the selective phenol synthesis with N_2O on a single alkali metal-ion site with a weak Lewis acidic character and without a redox property, we simulated a coordination structure of Cs^+ site at a cross channel arrangement in β zeolite pore and a reaction pathway involving the adsorption state and transition states for the selective oxidation of benzene to phenol with N_2O on the Cs^+/β cluster based on DFT calculations. The typical calculated structures for the reaction pathway are shown in Figure 3. The first step of the process is associated with benzene adsorption on the Cs^+ ion coordinated by a β zeolite cluster through the π bond. N_2O also adsorbs molecularly, which is rather in contrast to the typical redox catalysis such as dissociative N_2O adsorption to form active α-oxygen species on Fe/ZSM-5.[29, 30, 33–35] In the next step, the O–N(N_2O) bond dissociation and O–C(benzene) bond formation proceeds concertedly via two transition states (TS1 and TS2). Then, N_2 undergoes desorption. Finally, the H atom on the O–C carbon in the coordinated benzene on Cs^+ ion site migrates to the O atom to form phenol (proton transfer) via a transition state (TS3). In this reaction pathway, the single Cs^+ ion site with a large ion diameter of 0.334 nm provides an active platform capable of inter-adsorbate reaction, resulting in the molecular transformation from benzene with N_2O to phenol without the Cs^+ site undergoing a redox reaction. Figure S5 shows an overall computational downhill-energy reaction profile for the selective oxidation of benzene to phenol with N_2O on the Cs^+/β by DFT calculations. The reaction pathway reveals the concerted inter-ligand reaction mechanism involving associative coadsorption and two transition states. The concerted inter-ligand benzene–N_2O activation without dissociated species and the downhill energy sequence may be the origin of the remarkable selectivity (99.9%). After the O–C(benzene) bond formation on the Cs^+ ion the Cs^+–O–C(benzene) is transformed to Cs^+–phenol by hydrogen(proton) migration, which is the rate-determining step for the concerted benzene C–H functionalization to phenol synthesis with N_2O on the single Cs^+ ion site incorporated at a cross channel of β zeolite pore.

We have also calculated the system for Bz+N_2O on Na^+ site. The reaction profile is shown in Figure S6. Only a transition state TS1 for the N_2O dissociation and O-C(Bz) bond formation was found as a downhill process and an intermediate Bz*-O*-N_2*/Na^+ did not exist as a stable species. This is a distinguished difference between Cs^+ and Na^+. The difference in the cationic radius seems to be responsible to this difference. For the Na^+ case the bond distances from Na^+ tend to be shorter than the Cs^+ case, resulting in the intermediates and transition states with stronger interactions with Na^+/β. The adsorption energy of N_2O, desorption energies of N_2 and phenol, and activation energy for the phenol formation were larger for the Na^+ system than for the Cs^+ system. Totally, the Na^+/β should also be active for the Bz+N_2O reaction toward the phenol synthesis though it is less active than the Cs^+/β.

Phenol desorption energies were calculated to be 4.9 kJ/mol for Cs^+ and 6.2 kJ/mol for Na^+, which are much smaller than 73.6 kJ/mol and 80.4 kJ/mol for the hydrogen migration as shown in Figure S5 and Figure S6, respectively. These small values enable phenol desorption to be easy, which allows the process to run as a catalytic cycle.

2.2 Selective oxidation of benzene with O_2 and NH_3 on single alkali and alkaline-earth metal-ion sites. Realizing direct phenol synthesis from benzene with O_2 in a single-step gas-phase flow reaction on a solid catalyst has long been one of the greatest challenges in the field of solid catalysis.[50] We examined whether the Rb/β and Cs/β catalysts that were active for the phenol synthesis from benzene with N_2O were capable of the benzene hydroxylation with O_2 at atmospheric pressure. However, the alkali metal ions were inactive for O_2 activation and no reactions of benzene with O_2 proceeded as typically seen in the case of Cs/β (Table 2; second entry). Recently, we reported that redox cluster catalysts such as Re_{10} cluster/ZSM-5, IrO_x cluster/β and $[NiO]_4$ cluster/β promoted benzene combustion to CO_2 with O_2, while phenol synthesis from benzene with O_2 proceeded in the presence of NH_3; although large amounts of NH_3 were consumed, the yields were low.[14, 15] In the current study we also examined the effect of the addition of NH_3 on benzene oxidation with O_2 and found that benzene C–H activation toward direct phenol synthesis in a three-components system (benzene+O_2+NH_3) proceeded with a high selectivity of 96.0% at 1.3% one-path conversion on 0.2 g of Cs(2 wt%)/β and Rb(2 wt%)/β at 593 K (Table 2). In particular, undesirable NH_3 consumption on the Cs//β was low (0.16% conversion) and was about one tenth of the 1.66% of free NH_3 oxidation in a two-components system (NH_3+O_2). Note that benzene remarkably suppressed the free NH_3 oxidation to N_2 on single Cs^+ ion sites in β pores by promoting a different reaction pathway toward the selective phenol synthesis. On the Re_{10}/ZSM-5, IrO_x/β and $[NiO]_4/\beta$, benzene was deeply oxidized to CO_2 with O_2, whereas on the single site Cs/β and Rb/β catalysts, no benzene oxidation with O_2 occurred. These results demonstrate that on the Cs/β and Rb/β, NH_3 promoted the benzene oxidation with O_2. It might be suggested that NH_3 was converted to N_2O with O_2 and the *in situ* formed N_2O was the active species; however, this suggestion was proven to be wrong as NH_3 was converted to N_2 with O_2, not to N_2O, NO and NO_2, on the Cs/β catalyst. Further, when a small amount of N_2O was added to a mixture

Table 2. Performances (conversion and selectivity) of various alkali and alkaline-earth metal/β zeolite catalysts and reference samples for the selective oxidation of benzene to phenol with O_2+NH_3 at 593 K [†]

Catalyst	Benzene conv./%	Phenol selec./%	NH_3 decomp. conv./%	$[NH_3]_{reacted}$/$[Phenol]_{produced}$
β zeolite	0	-	-	-
Cs(2 wt%)/β [a]	0	-	-	-
Cs(2 wt%)/β [b]	-	-	1.7	-
Cs(2 wt%)/β [c]	1.3	96.0	0.2	0.2
Rb(2 wt%)/β [c]	1.3	96.0	5.6	8.3
Cs(2 wt%)/ SiO_2-Al_2O_3 [c]	0.01	76.5	0.5	229
Cs(2 wt%)/β	5.9	83.4	1.5	1.1
Cs(2 wt%)/β [d]	6.3	85.1	1.0	1.9
Cs(2 wt%)/β [e]	6.8	77.5	1.1	2.2
Rb(2 wt%)/β	6.9	60.5	3.5	17.8
Na(2 wt%)/β	2.1	44.2	40.4	55.6
Mg(2 wt%)/β	1.2	55.4	3.5	114
K(2 wt%)/β	3.4	60.1	2.5	25.8
Ca(2 wt%)/β	2.3	69.9	2.6	33.5
Sr(2 wt%)/β	1.2	67.6	2.8	7.5
Ba(2 wt%)/β	3.5	62.0	3.9	38.9

[†] The catalysts were pretreated with benzene/O_2/NH_3/He=0.5/0.5/1.8/4 mL min^{-1} at 673 K for 0.5 h. Cat. = 0.6 g; Performance values: averaged during 30-180 min time-on-stream. Benzene/O_2/NH_3/He = 0.5/0.5/1.8/4.0 mL min^{-1}. $[NH_3]_{reacted}$/$[Phenol]_{produced}$: reacted NH_3 amount/produced phenol amount. TOF is defined as reacted benzene(mol)/total metal(mol)/h. Zeolite β was purchased from Nikki Co. [a] Benzene/O_2/He =1.0/0.4/5.8 mL min^{-1}. [b] O_2/NH_3/He =0.5/1.8/4.5 mL min^{-1}. [c] Cat.=0.2 g; Benzene/O_2/NH_3/He = 1.0/0.5/1.8/4.0 mL min^{-1}. [d] identical condition to [†] except reac. temp. 603 K. [e] identical condition to [†] except reac. temp. 623 K.

of benzene and NH_3, the benzene hydroxylation to phenol was negligible, thus indicating that the benzene oxidation with N_2O was inhibited by the coexisting NH_3. In the benzene+O_2+NH_3 reaction on the Cs^+/β only a product from NH_3 was N_2 and neither N_2O, NO nor NO_2 were observed. These results demonstrate that the selective phenol synthesis is ascribed to contribution of O_2 molecules. No benzene oxidation occurred in the presence of propyl amine and pyridine, which were added to the system instead of NH_3. The critical performance for direct phenol synthesis from benzene with O_2 under coexisting NH_3 for the practical application to an industrial process should exceed 5% one-path conversion and 70% selectivity, and the ratio of the amounts of the consumed NH_3 and the produced phenol is approximately less than 2.[14-16] Hence, we attempted optimizing catalyst fabrication and reaction conditions to achieve higher than the critical performance.

We examined the effects of the types of Cs precursors and zeolites on the oxidation catalysis. The catalytic performance largely depended on the types of Cs precursors ($CsNO_3$, Cs_2CO_3, CsCl and CsOH) and the source of zeolites (Zeolyst, JGC C&C, Tosoh and Clariant). $CsNO_3$ was the best precursor, while CsCl was the worst precursor. The difference may be due to the difference in the ionic or covalent character among the precursors. $CsNO_3$ is highly ionic and Cs ions can be effectively supported in the zeolite surface layers by an ion exchange method, while CsCl has a higher degree of covalency. Among the zeolite sources, highly crystalline β zeolite from JGC C&C showed the best performance as a support for Cs. Using Cs(2 wt%)/β zeolite (JGC C&C), we further synthesized phenol from benzene with O_2+NH_3. We achieved 5.9% benzene one-path conversion and 83.4% selectivity on 0.6 g of the Cs/β at 593 K and 6.9% benzene one-path conversion and 64.5% selectivity on 1 g of the Cs/β at 593 K (Table 2). No other liquid products were detected, and the only observed by-product was gaseous CO_2, which actually eliminated the problem of separating the product from the system. In the catalysis on 0.6 g Cs(2 wt%)/β at 593 K the lowest NH_3 consumption $[NH_3]_{reacted}/[phenol]_{produced}$ = 1.10 was achieved, while also yielding good performance. Next, we changed the reaction temperature for 0.6 g Cs/β, and realized 6.3% benzene one-path conversion and 85.1% selectivity at 603 K and 6.8% benzene one-path conversion and 77.5% selectivity at 623 K (Table 2). To the best of our knowledge, these are the highest yields for the direct phenol synthesis from benzene with O_2 in single-step gas-phase flow reactions, and there have been no reports on good benzene C-H activation toward phenol synthesis by alkali-metal based catalysts. Moreover, 2 wt %-Cs/β showed the best activity, and the increment in Cs loading reduced the phenol yield. The basicity of catalysts increased with an increment in the alkali loading and the effective charges of O atoms coordinated to alkali ions increased;[51] consequently, phenol desorption became difficult, resulting in deterioration of the performance.

We performed DFT calculations for the selective oxidation reaction pathway on Cs/β (Figure 4) to understand the origin of the unique property of the single Cs^+ site catalysis. A detailed computational reaction profile for the reaction mechanism involving associative coadsorption states and transition states for the selective oxidation of benzene to phenol with O_2 regulated by NH_3 on the Cs^+/β cluster by DFT calculations is shown in Figure S7. A simulated coordination arrangement for the molecular coadsorption of benzene, O_2 and NH_3 on a Cs^+ ion at the cross channel in the β zeolite pore is also shown in Figure 4 and in Figure S8; this arrangement conforms to the pore channel space of β zeolite. At the molecular coadsorption state, the adsorbed O_2 is activated with the coadsorbed NH_3 to dissociate O_2 and form an O–C (benzene) bond in a concerted mechanism via a transition state (TS1). The inter-coadsorbate reaction (three-molecular concerted mechanism) on a single Cs^+ site is a plausible explanation for the high phenol selectivity. Finally, the H atom on the O–C (benzene) carbon atom migrates to the oxygen atom (proton transfer) to form phenol via the second tran-

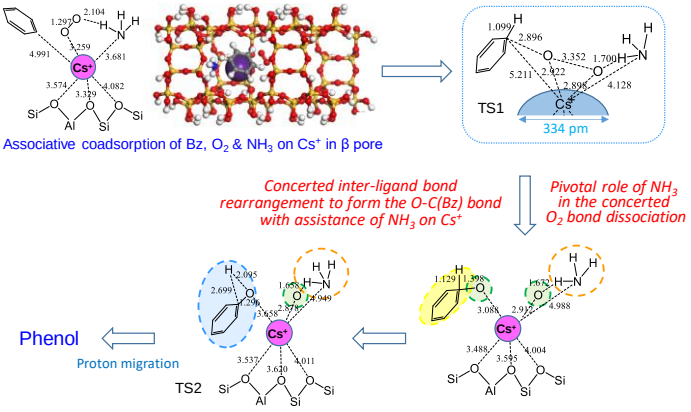

Figure 4. Associative Bz+O_2+NH_3 coadsorption, concerted O–C(Bz) bond formation assisted by NH_3 and transition states (TS1 and TS2) in a computational reaction pathway on single Cs^+ site at a cross channel in β zeolite pore.

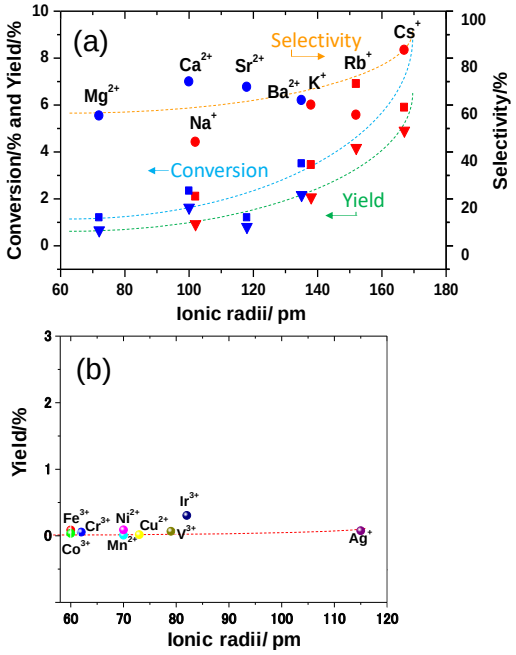

Figure 5. Relation between catalytic performances and ionic radii. (a) Plots of the benzene conversion(%), phenol selectivity(%), and phenol yield(%) versus the ionic radii of alkali and alkaline earth metal ions and (b) plots of the phenol yield(%) vs the ionic radii of transition and precious metal ions (Conv.% and selec.% are shown in Table S2). Reac. temp. = 593 K; Cat. = 0.6 g; Performance values: averaged during 30-180 min time-on-stream; Benzene/O_2/NH_3/He = 0.5/0.5/1.8/4.0 mL min^{-1}. Symbols in (a) [▪] : conversion of benzene; [●] selectivity to phenol; [▼] yield of phenol. Red symbols: alkali metals; blue symbols: alkaline earth metals.

sition state (TS2). There are double cascades (TS1 and TS2) in the energy profile. To summarize, DFT calculations indicate that the catalytic activity arises from the supported Cs cations in β pores and that the activation barriers are sufficiently moderate for the reactions to proceed at low temperatures in agreement with the experimental results. This reaction pathway proceeds on a single Cs^+ site; in other words, a large reaction platform is necessary on the Cs^+ site in the β pore. The ion diameters of Cs^+ (0.334 nm) and Rb^+ (0.304 nm) are significantly larger than the diameters of other alkali and alkaline earth metal ions. Therefore, this process can proceed on the single Cs^+ and Rb^+ sites.

Figure 5 shows the plots of the benzene one-path conversion (%), phenol selectivity (%) and phenol yield (%) against the ionic radii of alkali metal (Na, K, Rb, and Cs) and alkaline earth metals (Mg, Ca, Sr and Ba) ions (a) and for comparison, also transition and precious metal (V, Cr, Mn, Fe, Co, Ni, Cu, Ag, and Ir) ions (b). These transition and precious metal ions/β samples with ion diameters smaller than 0.240 nm did not show significant yields for phenol synthesis as compared to the yields of the alkali and alkaline earth metal ions/β catalysts, particularly Rb^+/β and Cs^+/β, with ion diameters greater than 0.300 nm. The single Rb^+ and Cs^+ sites cannot activate benzene, O_2, and NH_3 when they get adsorbed independently; however, when they coadsorbed together, the reaction of the inter-coadsorbates on the single metal site proceeded concertedly, causing benzene C-H activation toward phenol synthesis. This mechanism differs from the redox catalysis mechanism and acid–base catalysis mechanism involving clearly defined interaction modes.

3. CONCLUSION

We found that the single alkali and alkaline earth metal cations incorporated in β-zeolite pores selectively promote benzene C-H activation toward direct phenol synthesis (1) from benzene and N_2O and (2) from benzene, O_2 and NH_3 via a mechanism that differs from the traditional redox catalysis concept. Among the alkali and alkaline earth metal ions, Cs^+ and Rb^+ with ion diameters greater than 300 pm provided the pivotal single metal ion site platform with a sufficiently large coordination sphere at a confined cross channel in β zeolite pore for the selective inter-coadsorbate concerted reaction pathway. These findings present a new approach for designing of highly efficient selective C–H activation catalysis under mild conditions.

ASSOCIATED CONTENT

Supporting Information

Figures S1–S8 for *in situ* Rb K-edge XANES spectra, STEM-EDS maps, XRD, TPD of CO_2 and CH_3CN, computational reaction profiles for benzene+N_2O on Cs^+/β and Na^+/β and benzene+O_2+NH_3 on Cs^+/β, computanional coadsorption arrangement on a Cs^+ ion, and Table S1 for a list of performance data in literature, and Table S2 for transition and precious metal ions/β performances. This material is available free of charge via the Internet at http://pubs.acs.org.

AUTHOR INFORMATION

Corresponding Author

Yasuhiro Iwasawa, E-mail: iwasawa@pc.uec.ac.jp

Funding Sources

Grant-in-Aid for Scientific Research of JSPS/MEXT (16F16078 and 16F16383).

Notes

The authors declare no competing financial interests.

ACKNOWLEDGMENT

The study was supported by Grant-in-Aid for Scientific Research (16F16078and16F16383). S. G. and S. S. A. thank JSPS Postdoctoral Fellowship for foreign researchers. The XAFS measurements were performed with the approval of SPring-8 subject number 2016A7840, 2017A7840 and 2018A7840.

REFERENCES

1. Jordan, W.; van Barneveld, H.; Gerlich, O.; Boymann, M. K.; Ullrich, J. *Phenol in: Ullmann's Encyclopedia of Industrial Chemistry; Wiley,* **2000**. Doi:10.1002/14356007.a19_299.pub2.
2. Gimeno, M. P.; Soler, J.; Herguido, J.; Menendez, M. Use of Fluidized Bed Reactors for Direct Gas Phase Oxidation of Benzene to Phenol.*Ind. Eng. Chem. Res.* **2010**, *49*, 6810–6814.
3. Ertl, G.; Knözinger, H.; Schüth, F;Weitkamp, J., Eds.; *Handbook of Heterogeneous Catalysis*, 2nd ed.; Wiley-VCH: Weinheim, **2008**.
4. Horváth, I. T., Ed.; *Encyclopedia of Catalysis*; John Wiley & Son: New Jersey, **2003**.
5. Sels, B.; Van de Voorde, M., Eds.; *Nanotechnology in Catalysis*; Wiley-VCH: Weinheim, **2017**.
6. Cornils, B., Herrmann, W. A., Wong, C. H.;Zanthoffeds, H. W. *Catalysis from A to Z*; Wiley-VCH: Weinheim, **2013**.
7. Sels, B.;Kustov, L., Eds.; Zeolites and Zeolite-like Materials; Elsevier, **2016**.
8. Thomas, J. M.; Thomas W. J., Eds.; *Principles and Practice of Heterogeneous Catalysis*, 2nded; Wiley-VCH: Weinheim, **2015**.
9. Beller, M., Renken, A.; van Santen R. A., Eds.; *Catalysis, From Principles to Applications*; Wiley-VCH: Weinheim, **2012**.
10. Granger, P., Agbossou, F.;Ledoux, M. J. Catalysis: From Academic Research to Industrial Applications.*Comptes Rendus Chimie.* **2016**, *19*, 1143–1370.
11. Ruiz, P.; Delmon, B., Eds.;*New Developments in Selective oxidation by Heterogeneous Catalysis*; *Stud. Surf.Sci. Catal.*1st ed., *Vol.72*, Elsevier, **1992**.
12. Busca, G. Acid Catalysts in Industrial Hydrocarbon Chemistry.*Chem. Rev.* **2007**, *107*, 5366–5410.
13. Tanabe, K.; Hölderich, W. F. Industrial Application of Solid Acid–Base Catalysts.*Appl. Catal. A: Gen.* **1999**, *181*, 399–434.
14. Bal, R.; Tada, M.; Sasaki T.; Iwasawa, Y. Direct Phenol Synthesis by Selective Oxidation of Benzene with Molecular Oxygen on an Interstitial-N/Re Cluster/Zeolite Catalyst. *Angew. Chem. Int. Ed.***2006**, *45*, 448–452.
15. Wang, L.; Yamamoto, S.; Hayashizaki, K.; Nagamatsu, S., Malwadkar, S.; Sasaki, T.; Tada, M.;Iwasawa, Y. Selective Synthesis of Phenol from Benzene with O_2 by Switchover of the Reaction Pathway from Complete Oxidation to Selective Hydroxylation by NH_3 on Ir/β and Ni/β Catalysts. *ChemCatChem***2015**, *7*, 3248–3253.
16. Wang, L.; Yamamoto, S.; Malwadkar, S.; Nagamatsu, S.; Sasaki, T.; Hayashizaki, K., Tada, M.;Iwasawa, Y. Direct Synthesis of Phenol from Benzene and O_2, Regulated by NH_3 on Pt/β and Pt-Re/ZSM-5 Catalysts. *ChemCatChem***2013**, *5*, 2203–2206.

17. Smeets, P. J.; Woertink, J. S.; Sels, B. F.; Solomon, E. I.;Schoonheydt, R. A. Transition-Metal Ions in Zeolites: Coordination and Activation of Oxygen. *Inorg. Chem.* **2010**, *49*, 3573–3583.
18. Parmon, V. N.; Panov, G. I.; Uriarte, A.; Noskov, A. S. Nitrous Oxide in Oxidation Chemistry and Catalysis: Application and Production.*Catal.Today***2005**, *100*, 115-131.
19. Shiju, N. R.; Fiddy, S.; Sonntag, O.; Stockenhuber, M.; Sankar, G. Selective Oxidation of Benzene to Phenol over FeAlPO Catalysts using Nitrous Oxide as Oxidant. *Chem. Commun.***2006**, 4955–4957.
20. Yoshizawa, K.; Shiota, Y.; Yumura, T.; Yamabe, T. Direct Methane–Methanol and Benzene–Phenol Conversions on Fe–ZSM-5 Zeolite: Theoretical Predictions on the Reaction Pathways and Energetics. *J. Phys. Chem. B***2000**, *104*, 734–740.
21. Sarma, B. B.; Carmieli, R.; Collauto, A.; Efremenko, I.; Martin, J. M. L.; Neumann, R. Electron Transfer Oxidation of Benzene and Aerobic Oxidation to Phenol. *ACS Catal.***2016**, *6*, 6403–6407.
22. Acharyya, S. S.; Ghosh, S.; Tiwari, R.; Pendem, C.; Sasaki, T.; Bal, R. Synergistic Effect Between Ultrasmall Cu(II) oxide and $CuCr_2O_4$ Spinel Nanoparticles in Selective Hydroxylation of Benzene to Phenol with Air as Oxidant. *ACS Catal.***2015**, *5*, 2850–2858.
23. Ene, A. B.; Archipov, T.;Roduner, E. Competitive Adsorption and Interaction of Benzene and Oxygen on Cu/HZSM5 Zeolites. *J. Phys. Chem. C***2011**, *115*, 3688–3694.
24. Long, Z.; Zhou, Y.; Chen, G.; Ge, W.; Wang, J. C_3N_4-$H_5PMo_{10}V_2O_{40}$: A Dual-Catalysis System for Reductant-Free Aerobic Oxidation of Benzene to Phenol. *Sci. Rep.***2014**, *4*, 3651.
25. Kubacka, A.; Wang, Z.; Sulikowski, B.;Corberán, V. C. Hydroxylation/Oxidation of Benzene over Cu-ZSM-5 Systems: Optimization of the One-Step Route to Phenol.*J. Catal.***2007**, *250*, 184–189.
26. Panov, G. I.; Sheveleva, G. A.; Kharitonov, A. S.; Romannikov, V. N.;Vostrikova, L. A. Oxidation of Benzene to Phenol by Nitrous Oxide over Fe-ZSM-5 Zeolites. *Appl. Catal. A.***1992**, *82*, 31–36.
27. Panov, G. I. Advances in Oxidation Catalysis; Oxidation of Benzene to Phenol by Nitrous Oxide.*CATTECH***2000**, *4*, 18–31.
28. Hölderich, W. F. Environmentally Benign Manufacturing of Fine and Intermediate Chemicals.*Catal.Today***2000**, *62*, 115–130.
29. Ryder, J. A.; Chakraborty, A. K.; Bell, A. T. Density Functional Theory Study of Benzene Oxidation over Fe-ZSM-5.*J. Catal.***2003**, *220*, 84–91.
30. Hensen, E. J. M.; Zhu, Q.; van Santen, R. A. Selective Oxidation of Benzene to Phenol with Nitrous Oxide over MFI Zeolites: 2. On the Effect of the Iron and Aluminum Content and the Preparation Route. *J. Catal.* **2005**, *233*, 136–146.
31. Kollmer, F.; Harsmann, H.; Hölderich, W. F.$(NH_4)_2SiF_6$-Modified ZSM-5 as Catalysts for Direct Hydroxylation of Benzene with N_2O: 1. Influence of the Treatment Method.*J. Catal.***2004**, *227*, 398–407.
32. Centi, G.; Perathoner, S.; Arrigo, R.; Giordano, G.; Katovic, A.; Pedula, V. Characterization and Reactivity of Fe-[Al,B]MFI Catalysts for Benzene Hydroxylation with N_2O.*Appl. Catal. A***2006**, *307*, 30–41.
33. Cherniavsky, V. S.; Pirtuko, L. V.; Uriarte, A. K.; Charitonov, A. S.; Panov, G. I. On the Involvement of Radical Oxygen Species O^- in Catalytic Oxidation of Benzene to Phenol by Nitrous Oxide. *J. Catal.***2007**, *245*, 466–469.
34. Li, Y.; Feng, Z.; van Santen, R. A.; Hensen, E. J. M.; Li, C. Surface Functionalization of SBA-15-Ordered Mesoporous Silicas: Oxidation of Benzene to Phenol by Nitrous Oxide. *J. Catal.***2008**, *255*, 190–196.
35. Fellah, M. F., Onal, I.; van Santen, R. A. A Density Functional Theory Study of Direct Oxidation of Benzene to Phenol by N_2O on a $[FeO]^{1+}$-ZSM-5 Cluster. *J. Phys. Chem. C***2010**, *114*, 12580–12589.
36. Niwa, S.; Eswaramoorthy, M.; Nair, J.; Raj, A.; Itoh, N.; Shoji, H.; Namba, T.; Mizukami, F. A One-Step Conversion of Benzene to Phenol with a Palladium Membrane.*Science***2002**, *295*, 105–107.
37. Dittmeyer, R.;Bortolotto, L. Modification of the Catalytic Properties of a Pd Membrane Catalyst for Direct Hydroxylation of Benzene to Phenol in a Double-Membrane Reactor by Sputtering of Different Catalyst Systems.*Appl. Catal. A: Gen.* **2011**, *391*, 311–318.
38. Blatter, F.; Sun, H.;Vasenkov, S.; Frei, H.Photocatalyzed oxidation in zeolite cages.*Catal.Today***1998**, *41*,297-309.
39. Frei, H. Selective Hydrocarbon Oxidation in Zeolites.*Science* ***2006***, *313*, 309-310.
40. Pidko, E. A.; Mignon, P.; Geerlings, P.; Schoonheydt, R. A.; Van Santen, R. A. A Periodic DFT Study of N_2O_4 Disproportionation on Alkali-Exchanged Zeolites X. *J. Phys. Chem. C***2008**, *112*, 5510–5519.
41. Mignon, P.; Pidko, E. A.; Van Santen, R. A.; Geerlings, P.; Schoonheydt, R. A. Understanding the Reactivity and Basicity of Zeolites: A Periodic DFT Study of the Disproportionation of N_2O_4 on Alkali-Cation-Exchanged Zeolite Y.*Chem.Eur. J***2008**, *14*, 5168-5177.
42. Iwasawa,Y.; Asakura, K.; Tada, M. Eds.; XAFS Techniques for Catalysts, Nanomaterials and Surfaces; Springer: New York, **2016**.
43. Ravel, B.; Newville, M. ATHENA, ARTEMIS, HEPHAESTUS: Data Analysis for X-Ray Absorption Spectroscopy using IFEFFIT. *J. Synchrotron Rad.* **2005**, *12*,537–541.
44. Rehr, J. J.;Albers, R. C. Theoretical Approaches to X-Ray Absorption Fine Structure.*Rev. Mod. Phys.* **2000**, *72*, 621–654.
45. Newville, M.; Ravel, B.; Haskel, D.; Rehr, J. J.; Stern, E. A.;Yacoby, Y. Analysis of Multiple-Scattering XAFS Data Using Theoretical Standards. *Phys. B.* **1995**, 208–209.
46. Delly, B.From Molecules to Solids with the DMol3 Approach.*J. Chem. Phys.* **2000**, *113*, 7756–7764.
47. Perdew, J. P.;Wang, Y. Accurate and Simple Analytic Representation of the Electron-Gas Correlation Energy.*Phys. Rev. B.***1992**, *45*, 13244–13249.
48. Halgren, T. A.; Lipscomb, W. N. The Synchronous-Transit Method for Determining Reaction Pathways and Locating Molecular Transition States. *Chem. Phys. Lett.* **1997**, *49*, 225–232.
49. Shchukarev, A. V.; Korolkov, D. V. XPS Study of Group IA Carbonates.*Cent. Eur. J. Chem.* **2004**, *2*, 347–362.
50. Roduner, E.; Kaim, W.; Sarkar, B.; Urlacher, V. B.; Pleiss, J.; Gläser, R.; Einicke, W. D.; Sprenger, G. A.; Beifuß, U.; Klemm, E.; Liebner, C.; Hieronymus, H.; Hsu, S. F.; Plietker, B.; Laschat, S.Selective Catalytic Oxidation of C–H bonds with Molecular Oxygen.*ChemCatChem***2013**, *5*, 82–112.
51. Duffy, J. A. Relationship between Cationic Charge, Coordination Number, and Polarizability in Oxidic Materials. *J. Phys. Chem. B***2004**, *108*, 14137–14141.

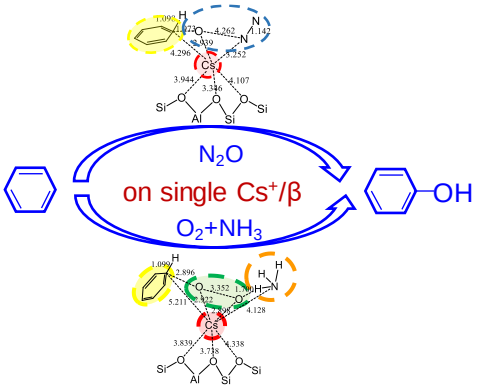
N2O
on single Cs+/β
O2+NH3
OH